

International Journal of Civil Engineering and Geo-Environmental

Journal homepage: <http://ijceg.ump.edu.my>
ISSN:21802742

NUMERICAL SIMULATION ON THE EFFECT OF KITCHEN HOUSE LOCATION AROUND RURAL HOUSE USING COMPUTATIONAL FLUID DYNAMICS

S. N. C. Deraman¹, T. A. Majid¹, S. S. Zaini^{1*}, W. Y. Tham¹, M. A. Ismail²

¹Disaster Research Nexus, School of Civil Engineering, Universiti Sains Malaysia, Engineering Campus, Penang, Malaysia

²Advance Packaging and SMT Group, School of Mechanical Engineering, Universiti Sains Malaysia, Engineering Campus, Penang, Malaysia

ARTICLE INFO

ABSTRACT

Keywords:

Windstorm
Pressure coefficient
Separation zone
Recirculation region

Most of the rural houses in the Northern region of Peninsular Malaysia are classified as non-engineered building. These rural houses are characterized by having overhang roof and kitchen house. There have been many cases of such houses being damaged during thunderstorm events. This study investigates the change in the distribution of pressure coefficient pattern around an isolated rural house model by varying the location of kitchen house. The roof pitch of core house, overhang and gap height was maintained at 27°, 0.5 m and 0.25 m in all cases, respectively. Computational fluid dynamics (CFD) simulations based on Reynolds-averaged Navier-Stokes equations (RANS) was used together with turbulence model, RNG k-ε. The influence of the position of the kitchen house on pressure coefficient distribution particularly true when the kitchen house was located on the windward side. The position of the kitchen house at the leeward side have no significant effect on the overall pressure distribution.

1. Introduction

Rural houses in Malaysia are mostly considered as low-rise non-engineered building which were constructed with a minimum or no structural engineering design (Muhammad et al., 2015). The characteristic of rural house in Malaysia is reflected with the presence of kitchen house or extension (rumah dapur) where this structure is built and attached to the core house (rumah ibu). Basically, kitchen house is built based on the free space of the surrounding. It can be at the windward or leeward area.

In Malaysia, windstorm occurrences keep increasing from year to year since 2010 to 2013 (Majid et al., 2016). The location of kitchen house can cause the change of wind flow. The study on the wind pressure distribution surrounding a structure can be carried out either experimentally using wind tunnel test or numerically using computer simulations. It cannot be denied that the wind tunnel test is more effective and

accurate, but can be time consuming and costly. On the other hand, Computational Fluid Dynamics (CFD) analysis has been successfully used by researchers to evaluate the interaction between wind and structures numerically (Huang et al., 2007; Irtaza et al., 2015). The objective of this study is to investigate the change in the distribution of pressure coefficient pattern around an isolated rural house model by varying the location of kitchen house.

2. Problem Statement

Malaysia is a country that experiences windstorm event. These events had caused damages to a number of houses especially at the roof of the core house. Roof uplift commonly happened to the non-engineered houses in rural area. This study aims to simulate wind pressure coefficient distribution on the roof with the changes of kitchen house location in order to determine the change in terms of pressure distribution an isolated rural house.

*Corresponding author. Tel: 04-5996221; Fax: 04-5941009

*Email address: ceshaharudin@usm.my

3. Methodology

An isolated gable-roof of core house with attached kitchen house was generated and the schematic view of the 3D building model used in the study is shown in Figure 1. The eave height (H_e), width and length was 4 m, 8 m and 12 m, respectively. These dimensions were obtained from (Zaini et al., 2016) where the best ratio was proposed to be 3:2:1 representing the length, width and height of the house, respectively.

The constant parameter such as 27° roof pitch, 0.5 m of overhang and 0.25 m of gap height model was used and tested with four different locations of kitchen house namely, edge windward, centre windward, edge windward and centre leeward. The mean streamwise velocity approaching flow was set at 26.4 m/s. The shape of the model was relatively similar to the typical rural house in the Northern region of Peninsular Malaysia as shown in Figure 1 (a). The plan view of rural houses are shown in Figure 1 (b) for the kitchen house located at the edge of the core house while Figure 1 (c) for the kitchen house located at the centre of the core house.

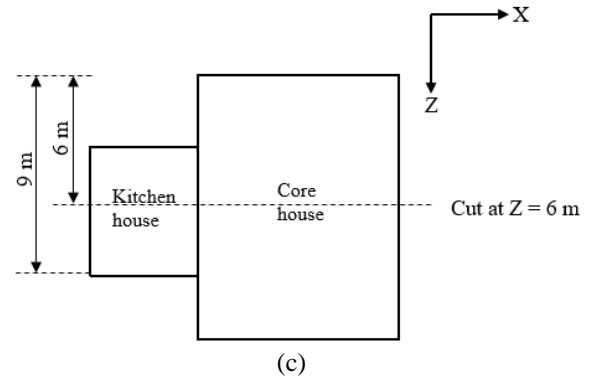
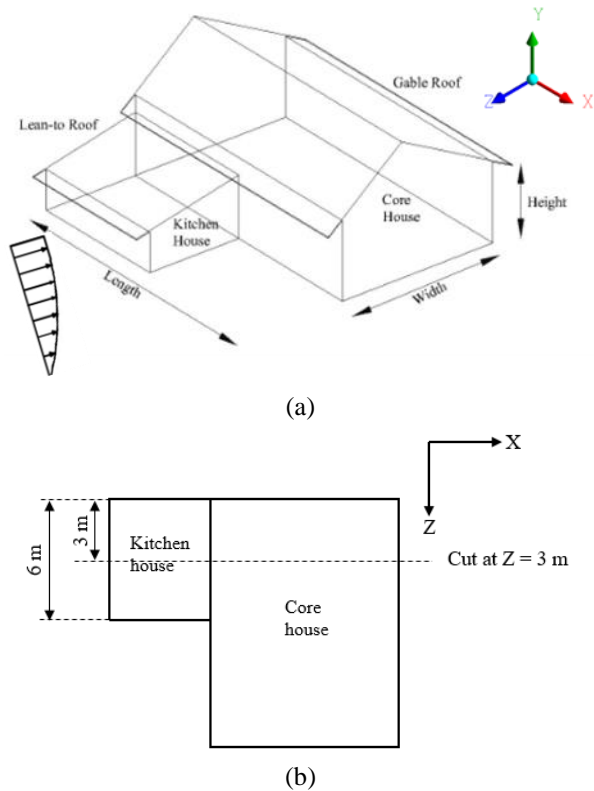


Figure 1: (a) Schematic view of rural house (b) plan view for kitchen house at the edge (c) plan view of kitchen house at the centre

3.1 Computational Method

In order to perform the steady-RANS equation, ANSYS Fluent 14.0 was used. This software is based on finite volume method for solving the flow equation with the capacity of dealing both structured and unstructured grids in its solver. RNG k- ϵ model was applied following the recommendations from Tominaga et al. (2015). Standard wall functions were applied to the wall boundaries (Lauder and Spalding, 1974). The second order implicit scheme was used for time discretization while the second order upwind discretization scheme was used to obtain higher accuracy. The SIMPLE algorithm was used for pressure-velocity coupling.

The computational domain size and boundary conditions was set as shown in Figure 2. The size of computational domain for lateral and the top boundary was recommended by Mochida et al., (2002), Shirasawa et al., (2003) and Tominaga et al., (2008) while the outlet boundary was set to be at least $10H_e$ behind the building model as suggested by Tominaga et al. (2008).

The boundary condition followed the setup from Tominaga et al. (2015). The inlet boundary condition was set as vertical wind profile of streamwise velocity and obeyed a power law relationship with an exponent of $1/7$, corresponding to an open terrain category. The vertical wind profile, turbulent kinetic energy and turbulent dissipation rate were incorporated into the algorithm via User Define Function (UDF). Likewise, the outlet boundary condition from the domain imposed zero static pressure and need to be placed far from the region where the influence of the target house was negligible. The upper and side of the domain was set as symmetry boundary conditions, implying zero normal velocity and zero gradients for all the variables at these boundaries (Tominaga et al., 2015). The boundary condition corresponding to the actual ground surface

was used with roughness height, $k_s = 0.035$ m and roughness constant, $C_s = 0.6$.

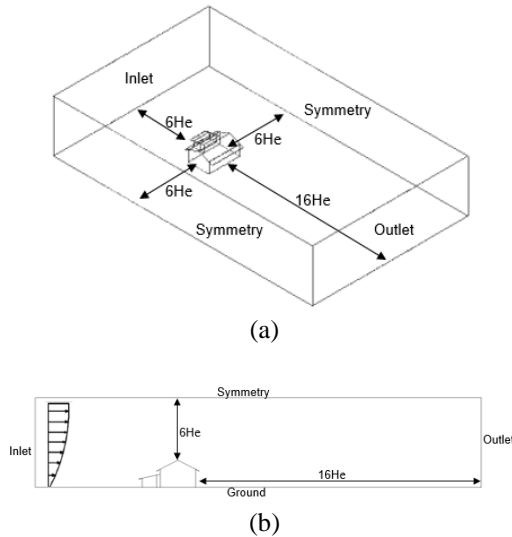


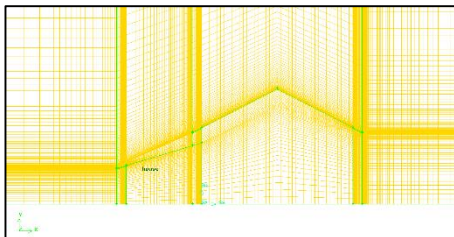
Figure 2: Dimension of the computational domain in (a) 3D view and (b) side view

The computational grid consisted 6,867,000 cells for the domain for all models. The average y^+ value over the windward and the leeward roofs were about 21 and 30.

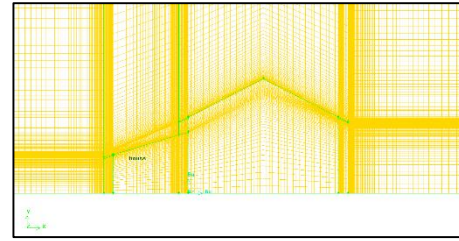
4. Results and Discussion

4.1 Grid-sensitivity analysis

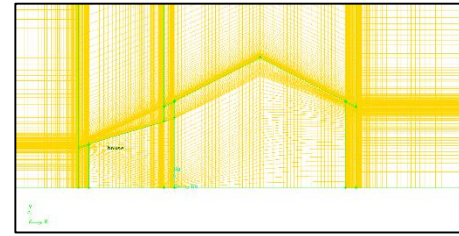
A grid-sensitivity analysis was performed based on two additional number of grids which are a coarse grid (6,053,400 cells) and a fine grid (7,812,000 cells). The average y^+ value for the coarse grid over the windward and the leeward roofs were about 100 and 50 while for the fine grid were 10 and 5. Figure 3 shows that the view of three different sizes of grids which are coarse, medium and fine grid.



(a)



(b)



(c)

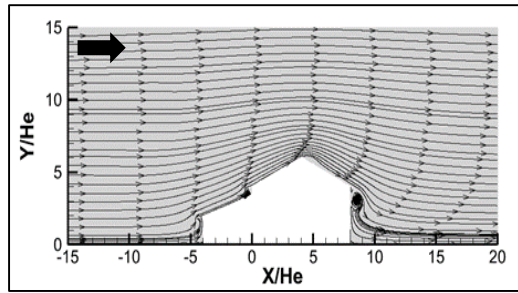
Figure 3: View of grids for grid-sensitivity test: (a) Coarse grid; (b) Medium grid; (c) Fine grid.

4.2 Streamline

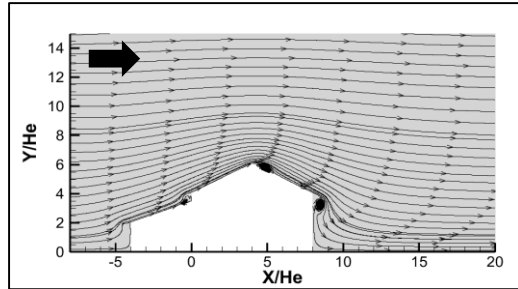
Figure 4 shows the streamline patterns for rural house models with different kitchen house configurations. Figure 4(a) and (c) were cut at $Z = 3$ m from the origin (as shown in Figure (b) while Figure 4(b) and (d) were cut at $Z = 6$ m from the origin (as shown in Figure 1 (c)). In general, it can be seen that the recirculation regions were spotted in front of the windward roof and beneath the overhangs. This is due to the fact that as the airflow approaches the wall, the pressure rise slightly with respect to the increase (positive) pressure built up thus reducing the wind speed. With the position of the kitchen house in the windward, the formation of eddies were relatively small compared to kitchen house position in the leeward direction.

The recirculation region at the ridge of the roof has the same pattern since the roof pitch for all cases are same. There is a complicated interaction between the eddy that occurred at the ridge and the recirculation flow formed by the entire house.

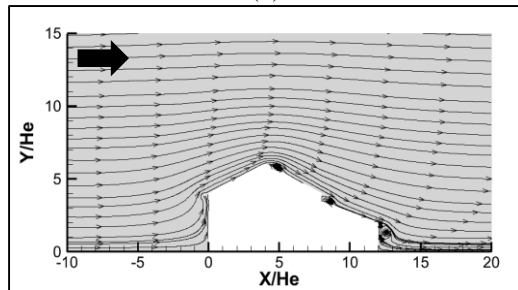
The flow pattern of reverse flow and formation of eddies were quite different for different position of the kitchen house. In general, the eddy was formed about the same level as the roof height in all cases.



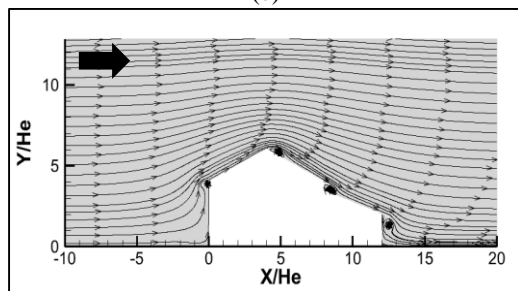
(a)



(b)



(c)



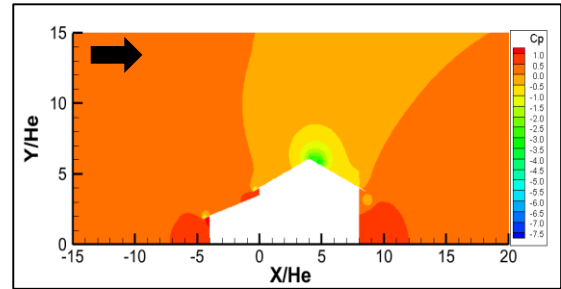
(d)

Figure 4: Streamline flow for different location of kitchen house (a) Edge windward (b) Centre windward (c) Edge leeward (d) Centre leeward

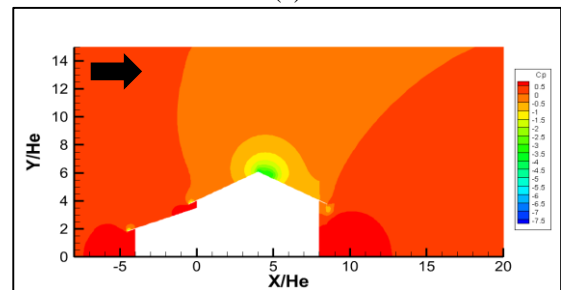
4.2 Spatial distribution of pressure coefficient

The pressure coefficient distribution on the kitchen house region at the windward were positive as shown in Figure 5(a) and (b). This finding can be associated to the formation of eddy at the windward wall and beneath the overhangs.

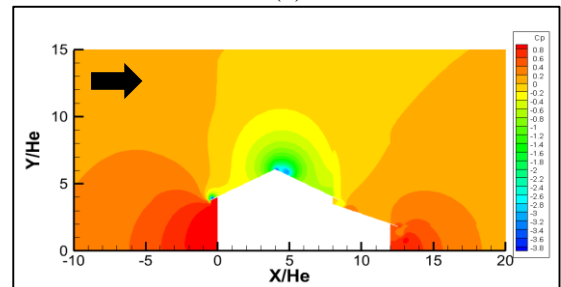
The maximum negative C_p (suction) were observed on the ridge of the core house due to the formation of the separation zone right after the ridge. The negative pressure was distributed uniformly about the same magnitude throughout the leeward wall. This phenomenon may be due to the occurrence of wake region after the separation zone.



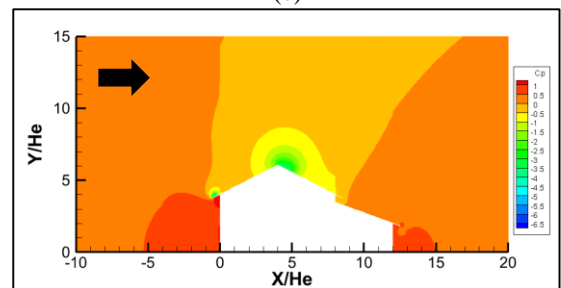
(a)



(b)



(c)



(d)

Figure 5: Pressure coefficient for different location of kitchen house (a) Edge windward (b) Centre windward (c) Edge leeward (d) Centre leeward

Peak negative pressure at $Z = 3$ m from the origin (as shown in Figure 1 (b)) was observed when the kitchen house was at the edge of the windward side as shown in Figure 5(a). Low positive pressures were formed closed to the overhang as there was no separation zone at the leading overhang. Hence, the wind pushed upward the lower part of the upwind roof for all cases.

There are negative pressure (suction) occurred at the upper side of the overhang for all cases. However, the highest suction occurred when the kitchen house was located at the leeward side as shown in Figure 5(c) and (d). This trend is formed due to the presence of the gap height at the windward side of the house. The large recirculation region occurred underneath the overhang as shown in Figure 5(c) and (d), hence generating high suction at the upper side of the leading overhang.

5. Conclusions

In this study, the air flow around isolated gable roof of rural house with different locations of kitchen house were investigated by CFD simulation based on steady-RANS.

It can be concluded that the lowest suction at roof ridge and leading overhang roof of the core house occurred when the kitchen house was located at the edge of the core house facing the leeward direction.

The influence of the position of the kitchen house on the distribution of pressure coefficient was significant when the kitchen house was located on the windward side which caused high suction at the ridge of the core house while high suction occurred at the upper side of the leading overhang which caused roof uplift when the kitchen house at the leeward side (no significant effect).

Acknowledgement

The authors express their gratitude for the financial support of the Fundamental Research Grant Scheme (FRGS) from the Ministry of Higher Education Grant (203.PAWAM.6071317), and the MyBrain15 Scholarship scheme from the Ministry of Education Malaysia.

References

- Mochida, A., Tominaga, Y., Murakami, S., Yoshie, R., Ishihara, T. and Ooka, R. (2002). 'Comparison of various $k-\epsilon$ models and DSM applied to flow around a high-rise building—Report on AIJ cooperative project for CFD prediction of wind environment,' *Wind Struct.*, 5(2-4), pp. 227–244.
- Launder, B.E. and Spalding, D.B. (1974). 'The numerical computation of turbulent flows,' *Computer Methods in Applied Mechanics and Engineering*, 3(2), pp. 269-89.
- Irtaza, H., Javed, M.A. and Jameel, A. (2015). 'Effect on wind pressures by variation of roof pitch of low-rise hip roof building,' *Asian J. Civ. Eng. (BHRC)*, 16(6), pp. 869-889.
- Muhammad, M.K.A., Majid, T.A., Ramli, N.I., Deraman, S. N. C. and Wan Chik, F.A. (2015). 'An Overview of Non – Engineered Buildings Roofing System failure under Wind Loads,' *Awam International Conference on Civil Engineering*, Kuala Lumpur.
- Huang, S., Li, Q.S. and Xu, S. (2007). 'Numerical evaluation of wind effects on a tall steel building by CFD,' *J. Constr. Steel Res.*, 63, pp. 612-627
- Zaini, S.S., Majid, T.A., Deraman, S.N.C., Wan Chik F.A. and Muhammad, M.K.A. (2016). 'Post windstorm evaluation of critical aspects causing damage to rural houses in the Northern region of Peninsular Malaysia,' *International Symposium Civil and Environmental Engineering*, Melaka.
- Shirasawa, T., Tominaga, T., Yoshie, R., Mochida, A., Yoshino, H., Kataoka, H. and Nozu, T. (2003). 'Development of CFD method for predicting wind environment around a high-rise building part 2: the cross comparison of CFD results using various $k-$ models for the flowfield around a building model with 4:4:1 shape,' *AIJ J. Technol. Des.*, 18, pp. 169-174.
- Tominaga, Y., Mochida, A., Yoshie, R., Kataoka, H., Nozu, T., Yoshikawa, M. and Shirasawa, T. (2008). 'AIJ guidelines for practical applications of CFD to pedestrian wind environment around buildings,' *J. Wind Eng. Ind. Aerodyn*, 96, pp. 1749–1761.
- Tominaga, Y., Akabayashi, S-I., Kitahara, T. and Arinami, Y. (2015). 'Air flow around isolated gable-roof buildings with different roof pitches: Wind tunnel experiments and CFD simulations,' *Build. Environ.*, 84, pp. 204-213